ARPHA Preprints

PENSOFT

PREPRINT

Author-formatted, not peer-reviewed document posted on 21/02/2025

DOI: https://doi.org/10.3897/arphapreprints.e150955

The role of the climate niche in repeated abrupt tree declines and ecotone dynamics in the Appalachian Mountains during the Holocene

Bryan Shuman, Ivanka Stefanova, Ioana C. Stefanescu, Tessa Ray-Cozzens, Jonathan Johnson, David M. Nelson

The role of the climate niche in repeated abrupt tree declines and ecotone dynamics in the Appalachian Mountains during the Holocene

Bryan N. Shuman[1], Ivanka Stefanova[2], Ioana C. Stefanescu[1], Tessa Ray-Cozzens[1], Jonathan Johnson[3], David M. Nelson[3]

1 Department of Geology and Geophysics, University of Wyoming, Laramie WY 82071

2 Department of Earth and Environmental Sciences, University of Minnesota, Minneapolis, MN 55455

3 Appalachian Laboratory, University of Maryland Center for Environmental Science, Frostburg MD 21532

Main text: 7217 words

Abstract (250 words)

Forests in eastern North American did not achieve a stable composition during the Holocene. Both prolonged and abrupt shifts in the distributions of tree species were common. Studying the dynamics involved can help anticipate the responsiveness of forest biogeography to climate change today. Here, we evaluate changes in two >12,000-year fossil pollen stratigraphies from the Appalachian Plateaus Province, Pennsylvania. They show repeated episodes of forest turnover following the widespread collapse of hemlock (*Tsuga canadensis*) populations at ca. 5000 years before present (YBP). The changes from 5000-2500 YBP include abrupt declines in taxa such as birch (*Betula* spp.) and beech (*Fagus grandifolia*), which produced unique forest phases each lasting 300-500 years. Emergent communities included the resurgence of oak (*Quercus* spp.) and white pine (*Pinus strobus*), which had been important several thousand years earlier. Two oak maxima at 4800-4250 and 3800-3200 YBP mark northward shifts in the regional oak-hardwood ecotone known as the “Tension Zone” and involve centennial-scale droughts during a millennial-scale period of warming. The changes, like those elsewhere along the ecotone from Ontario to Massachusetts, differ from successional dynamics that might have been expected after the hemlock decline. Instead, the forest histories included abrupt changes, short-lived communities, and asynchronous changes across sites consistent with the interaction of a) individualistic species’ climate niches and b) multiple scales of climate variation. Comparison of the pollen records with heuristic forest history simulations demonstrates that landscape-scale forest changes, integrated across mosaics of many stands, match patterns expected from deterministic, equilibrium responses to climate change.

Keywords: Holocene, pollen, forest, ecotone, abrupt change, Appalachian, Pennsylvania

Introduction

Paradoxically, abrupt forest changes (<500 yr) were common during the ostensibly 'stable' climates of the Holocene Epoch of the past 11,700 years (Shuman et al. 2009, Seddon et al. 2015). Evaluating the processes that shaped these abrupt changes can help to anticipate future ecosystem outcomes of anthropogenic climate change (Williams et al. 2011, Jackson and Blois 2015). Fossil pollen stratigraphies from the northeast U.S. (Fig. 1) provide a particularly useful case because they document a rich sequence of forest changes, which developed in the context of millennial and centennial climate variability (Fig. 2). Past work has examined many of the long-term (>1000 yr) features of the regional forest history (Watts 1979, Oswald et al. 2020), which generally maintained a dynamic equilibrium with climate (Shuman et al. 2004, Shuman et al. 2009, Shuman et al. 2019). However, the details of the stratigraphies also indicate centennial-scale variations, including abrupt tree declines (e.g., Clifford and Booth 2015), which may reflect the interactions between intrinsic forest processes like disturbance and succession and externally-driven responses to the regional climate history (Fuller 1998, Williams et al. 2011, Shuman et al. 2019). The changes were short lived, but are relevant to changes playing out over decades today and may have altered first-order biogeographic patterns such as the northeastern U.S. forest ecotone, known as the 'Tension Zone' between northern hardwoods (green-yellow in Fig. 1) and southern oak-hickory (*Quercus-Carya*) forests (tan in Fig. 1)(Cogbill et al. 2002, Thompson et al. 2013, Paciorek et al. 2016).

The northeastern Tension Zone has a dynamic Holocene history related to climate changes, disturbance, and species immigration (Fuller et al. 1998, Foster et al. 2002, Thompson et al. 2013, Oswald et al. 2018). Changes included a rapid, range-wide decline of the eastern hemlock

(*Tsuga canadensis*) populations that help to define it (yellow, Fig. 1). The decline at ca. 5000 years before present (YBP) has been well studied and debated (Davis 1981, Allison et al. 1986, Foster et al. 2006, Booth et al. 2012), but additional, potentially related, centennial-scale variations also affected forest composition at Tension Zone sites from Massachusetts to Ontario and have not been specifically evaluated (Fuller 1998, Oswald et al. 2007, Oswald et al. 2018). These and other rapid changes do not represent responses to the slowly varying, long-term drivers of regional climate change (Fig. 2A)(Davis 1981, Fuller 1998). They may have been shaped, however, by the interaction between species' climate niches (Prentice et al. 1991, Williams et al. 2006) and additional fluctuations in regional temperature or moisture gradients (Fig. 2B-C)(Yu et al. 1997, Foster et al. 2006, Marsicek et al. 2013, Shuman et al. 2023, Stefanescu et al. 2023). Such fluctuations include centennial variations recorded by a) pollen-inferred precipitation reconstructions (green line, Fig. 2C)(Shuman et al. 2019), b) physical indicators of water-level changes traceable across multiple lakes (dark blue line, Fig. 2C)(Newby et al. 2014), and c) alkenone-inferred sea-surface temperatures (light blue line, Fig. 2C)(Sachs 2007). Any consequences of this centennial climate variability must have also interacted with the impacts of forest diseases (Allison et al. 1986), insect outbreaks (Anderson et al. 1986, Bhiry and Filion 1996), extreme weather events (Foster and Boose 1992, Pederson et al. 2014), and human use of wildfire (Maenza-Gmelch 1997, Nowacki and Abrams 2008, Nowacki and Abrams 2015), although evidence of such disturbances is often not present in association with the abrupt vegetation changes (Foster et al. 2006, Oswald et al. 2016, Oswald et al. 2020). The regional arrival of new tree species, such as American chestnut (*Castanea dentata*), at different points during the Holocene likely further altered the pathways of forest change (Foster and Zebryk 1993, Foster et al. 2002).

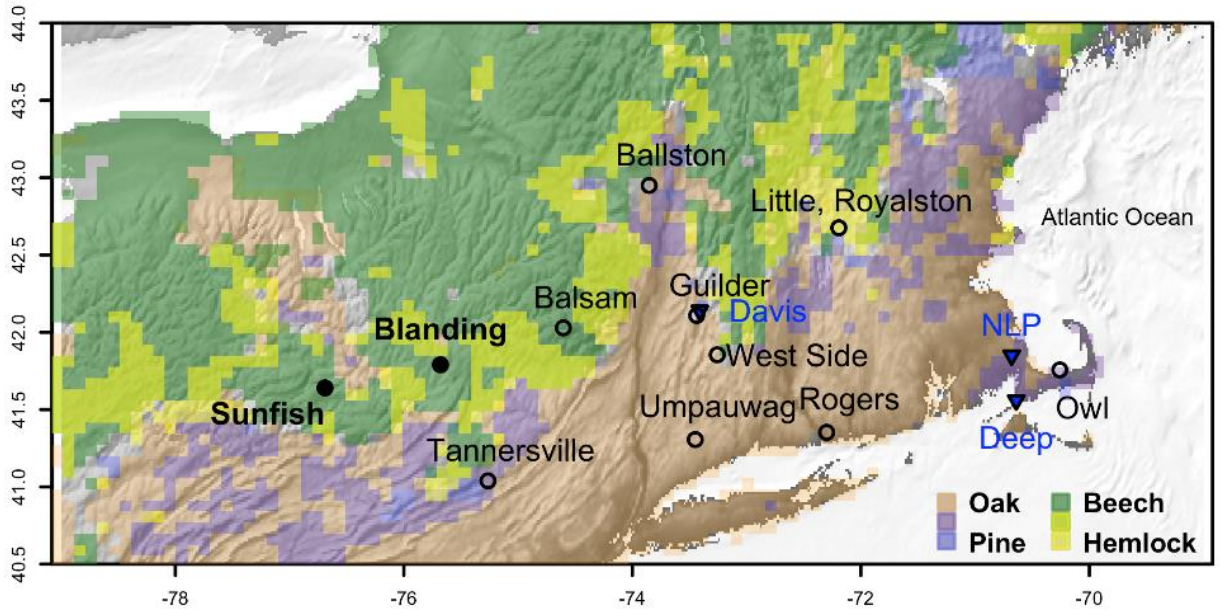

Figure 1. Historic distributions of forests with >20% oak, pine, beech or hemlock trees in the northeast U.S. with the locations of fossil pollen (circles) and lake level (blue triangles) study sites discussed here. The focal study sites are shown in bold with filled black circles. NLP refers to New Long Pond. Tree distribution data from Paciorek et al. (2016).

A challenge for understanding the centennial-to-millennial timescales of forest variation arises, therefore, from uncertainty about how the effects of climate variation interacted with those of the repeated disturbances, successional trends, and the arrival of new taxa that shaped whole pollen source areas (landscapes) on similar timescales (Anderson et al. 1986, Fuller 1998, Ramiadantsoa et al. 2019). Several hypotheses about forest variability in the mid-Holocene illustrate the range of potential dynamics. An important initial null model is that centennial forest variably, even including abrupt tree declines, arose at the scale of pollen source areas from a dynamic equilibrium between a ‘steady state mosaic’ averaged over the forested landscape and the fluctuating regional climate; i.e., the mean outcome of many individual forest stands closely

tracked the mean climate trends as determined by species climate niches (Webb 1986, Prentice et al. 1991, Shuman et al. 2019).

However, a range of processes could have modified this dynamic. First, the range-wide hemlock decline, regardless of its cause, may have initiated successional dynamics across the region, which would appear as distinct centennial-scale forest phases in Holocene pollen records (Fuller 1998). Second, sequences of compounded large disturbances, such as successive severe droughts (Shuman and Burrell 2017)(Fig. 2C), could have also generated centennial-scale forest phases by triggering asynchronous abrupt declines with the most sensitive taxa (e.g., hemlock) declining immediately followed later by other taxa stressed by previous events (Paine et al. 1998, Turner et al. 2019). Large disturbances in sequence can, in this way, disrupt the emergence of a 'steady state' in the regional forest mosaic (Baker 1989, Turner et al. 1993). Finally, stochastic extreme events and autoregressive population processes likely create complex forest trajectories at forest stand scales, which may scale up to produce centennial-scale regional outcomes contingent on the sequence of events rather than closely tracking the shifting mean climate (Jackson et al. 2009, Pederson et al. 2014, Ramiadantsoa et al. 2019).

Here, we consider the relevance of the null model and the alternate hypotheses to centennial forest variation and repeated abrupt tree declines near the Tension Zone in the Appalachian Plateau Province of Pennsylvania. We focus on forest changes from 5000-2500 YBP when the hemlock decline and additional related changes took place (Davis 1981, Fuller 1998, Foster et al. 2006, Shuman et al. 2023). For context, we use simple heuristic simulations to demonstrate the null model by calculating how climate niches could directly determine responses to Holocene

120 climate variability. We then identify the patterns and timescales of forest composition and
121 turnover in two new fossil pollen stratigraphies and compare them with our simulations, with
122 examples of known successional changes (e.g., Brugam 1978), and with the regional climate
123 history including repeated droughts (Fig. 2).

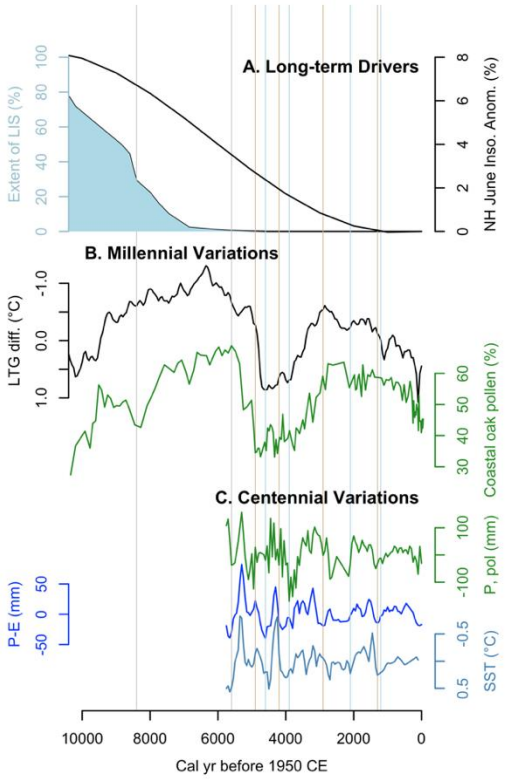

*Figure 2. Paleoclimate variations in the northeast U.S. include responses to **A)** long-term drivers of change, **B)** millennial variations, and **C)** centennial fluctuations. Long-term drivers (A) include the extent of the Laurentide Ice Sheet (LIS) (Dyke, 2004) and seasonal insolation anomalies in the northern hemisphere (Berger and Loutre, 1991). Two datasets with no direct interdependence show the millennial pattern in (B): a reconstruction of the regional latitudinal (north-south) temperature gradient (LTG diff.) based on data from >30 lakes (black line; Shuman et al., 2023) and changes in temperature-sensitive coastal oak (Quercus) populations on Cape Cod, Massachusetts (green line; Foster et al., 2006). Detrended datasets also preserve centennial-scale anomalies (C) in pollen-inferred precipitation (P, green line, Shuman et al., 2019), lake-level derived precipitation minus evaporation (P-E, blue line, Newby et al., 2014; Shuman et al., 2019), and sea-surface temperatures (light blue) (Sachs, 2007). LTG refers to latitudinal temperature gradient. Vertical lines mark the beginning (orange) and end (blue) of periods of low lake levels (Newby et al., 2014) and 8200 and 5800 YBP (gray).*

124

125 **Study Sites**

126 The two study sites, Blanding Lake and Sunfish Pond, sit within the highlands of Pennsylvania
127 (Fig. 1). Both are located near the Tension Zone in forests populated historically by hemlock,
128 beech (*Fagus grandifolia*), multiple maple species (*Acer* spp.), and various birches (*Betula*
129 spp.)(Cogbill et al. 2002, Thompson et al. 2013, Paciorek et al. 2016). Blanding Lake (41.79°N,
130 75.68°W, 454 m elevation, 4.8 ha, 555 cm maximum water depth) is one of many similar sized
131 lakes located amid rolling hills and steep-sided valleys of the Delaware-Neversink Highlands in

Susquehanna Co., Pennsylvania (Sevon 2000). July temperatures at the lake currently have a mean of 20.0°C while January has a mean of -5.7°C; mean annual temperature and precipitation equal 7.5°C and 1175 mm, respectively (PRISM Climate Group 2022). The landscape surrounding Blanding Lake contains a nearly even mix of managed deciduous forests and cleared agricultural areas. The lake itself sits within a small primarily forested watershed (45 ha) defined by hills and ridges reaching to ~500 m elevation above sea level. Previous work showed that the lake level fluctuated repeatedly since the lake's formation ca. 15,000 YBP with low water episodes from 5500-3800 and 2800-2000 YBP (Shuman and Burrell 2017).

Sunfish Pond (41.64°N, 76.69°W, 635 m elevation, 11 ha, 585 cm maximum depth) is a glacially formed lake, located on a ridge crest in the Allegheny Mountains in Bradford County, Pennsylvania. The local climate is similar to that at Blanding Lake with mean annual, July and January temperatures of 7.5, 19.9 and -5.5°C, respectively, and mean annual precipitation of 1140 mm (PRISM Climate Group 2022). The 1.1 km^2 watershed drains an area of low relief on top of LeRoy Mountain within the Glaciated High Plateau region (Wood 1911, Sevon 2000). Steep, northwest facing mountain slopes north of the lake descend >300 m in elevation in <2 km to the reach the Low Plateau region, which includes low-elevation hilly terrain where the Newton Mammoth Site is located at Spring Lake (Barnosky et al. 1988) and which is crossed by the Susquehanna River. European settlement of Bradford County around Sunfish Pond dates to CE 1760, but population density is low near the lake (Wood 1911) and Pennsylvania State Game Management Lands have conserved the lake watershed and surrounding areas as forest.

Soils differentiate the two lakes. The Volusia-Morris soil series, a group of deep, moderately drained soils in loamy till, surround Blanding Lake (Reber 1973, USDA Natural Resources Conservation Service 2016), which occupies a depression within the Pleistocene Orlean Till over sandstones of the Devonian Catskill Formation (Berg et al. 1980, Sevon and Braun 1997, Braun 2011). At Sunfish Pond, however, only thin glacial till and scattered glacial erratics cover the underlying bedrock, composed of the Pottsville Formation, a gray sandstone and conglomerate (Myers 1954). The local Lordstown soil series is composed of well-drained soils formed in till and cryoturbated fragments of the underlying siltstone and sandstone (USDA Natural Resources Conservation Service 2016).

Methods

Simulations

We use simulations of three idealized taxa and their responses to decadal to multi-millennial climate variations to demonstrate how species' climate niches might shape centennial-scale vegetation responses to climate at the landscape scale. The premise underlying the simulations derives from theory and observations about climatic niches: processes from regeneration to competition define a unimodal climatic optimum for most tree species, which represents how the sum of these processes determines each taxon's response to climate variations (Grubb 1977, Prentice et al. 1991, Peterson et al. 2011). Most niches exist in multiple dimensions defined by seasonal temperatures and moisture availability (Williams et al. 2006), but for our purposes, we simulate a simplified niche for our three idealized taxa based on a single arbitrary 'climate' index (Fig. 3A-C).

The simulations include two key equations, calculated in R (R Core Development Team 2022). First, each pseudo-species has an abundance that is (in this simplified model) deterministically based on the climate index at time T (C_t), such that between two limits (C_{min}, C_{max}), the abundance represents a single sine wave with a fixed mode (C_{mode}) and breadth ($C_{breadth}$):

$$\text{For } C_t > C_{min} \ \& \ C_t < C_{max}: \qquad A_t = \sin(0.5+((C_t - C_{mode})/C_{breadth})) \tag{1}$$

When the value of the climate at any point in time (C_t) falls outside of the two limits, the abundance (A_t) becomes zero.

Second, we assume that tree growth and successional processes delay the immediate response of each taxon's abundance to the changing climate. To account for the lagging changes, we apply the concept of an 'e-folding' response with a response time (λ), which represents the amount of time for ~63% of the response to develop (Webb 1986):

$$A_T = A_t + (A_{T-1} - A_t) * \exp(-t/\lambda) \tag{2}$$

Here, A_T and A_{T-1} represent the actual abundances at time T and T-1, and A_t represents the potential abundance determined by the niche at time T from equation 1. The time step of the model (t) used here is 20 years. We use 75 years for λ to approximate successional time scales (i.e., the duration of the first 63% of the changes) in Appalachian deciduous forests.

We apply the model to three pseudo-species with different climatic modes spread across a climate gradient spanning the magnitude of a synthetic 8000-year climate trend. We added a millennial oscillation and a second, smaller multi-century oscillation (i.e., two sine waves) to the trend (black line, Fig. 3D) as well as stochastic decadal variability (black lines, Fig. 3E-F). For comparison, we generated a first simulation without the stochastic decadal variability and then

two different simulations representing different 'sites' with the same mean climate trend and oscillations but different decadal variability (black and red lines, Fig. 3E-F). The stochastic decadal variability primarily represents atmospheric variability but could be considered to include site-level microclimate variations shaped by local disturbances and other forest ecosystem processes. Although the decadal variability is randomly drawn from a normal distribution, the simulated species responses are entirely deterministic following equations 1 and 2. The model, thus, represents an extreme, simplified form of the null model of potential climate-driven outcomes and their site-to-site variability, which we contrast with the two new pollen records.

Pollen stratigraphies

Cores were collected from the deepest point within each lake in 2015 from a floating platform using a hand-driven piston corer. Core sections were retrieved in sequential sections through the entire thickness of lake sediment (to refusal) in 1-m long, 70 mm diameter plastic tubes. The sections were refrigerated upon arrival at the University of Wyoming where they were split and sub-sampled in contiguous 1-cm intervals. All sub-samples were analyzed for loss-on-ignition (LOI) at 550°C for 2 hrs to estimate organic content (Shuman 2003).

Core chronologies were developed by sieving sub-samples to obtain macroscopic charcoal fragments for radiocarbon analyses. However, the Sunfish Pond core contained insufficient charcoal and 1-3 cm^3 bulk sediment samples were analyzed instead because the sediment was organic-rich and contained no carbonates, which are also absent from the watershed. Charcoal samples were analyzed by the W. M. Keck Carbon Cycle Accelerator Mass Spectrometer

Facility at the University of California, Irvine, and bulk sediment samples by National Ocean Sciences Accelerator Mass Spectrometry at the Woods Hole Oceanographic Institution. Resulting radiocarbon ages were calibrated using Intcal20 (Reimer et al. 2020) and age-depth models were generated using bchron (Haslett and Parnell 2008, Parnell et al. 2008). Resulting sample ages were cross compared across the two sites, to assess the quality of bulk sediment ages and detect outliers, by contrasting the timing of regionally significant features in their birch (*Betula*) and hemlock (*Tsuga*) pollen stratigraphies.

Pollen was processed and counted from selected sub-samples using standard techniques (Faegri and Iverson 1989). Samples were initially selected in each core at 15-20 cm intervals to provide ~300 yr sample resolution spacing based on the chronologies. Additional subsamples were added to the Sunfish Pond core from 8000-2800 YBP to increase temporal resolution to <130 yrs between samples. The samples were processed at the University of Wisconsin and then mounted on slides and counted under 40x magnification at LacCore at the University of Minnesota. On average, 500 individual palynomorphs were counted from each sample. Pollen percentages were calculated from the sum of terrestrial pollen types.

Constrained cluster analysis (CONISS)(Grimm 1987) was used to determine the location of major changes in the pollen assemblages within each stratigraphy; stratigraphically adjacent clusters were determined using Bray-Curtis dissimilarity among the percentages of taxa with >2% representation. The analysis was conducted using *chclust* in the *rioja* package in R and significance of the breaks were tested using *bstick* and plotted using *riojaPlot* (Juggins 2022, R Core Development Team 2022). Low-frequency variations in the time series of individual taxa

were estimated using the *loess* function in base R with smoother spans equal to 0.5 (5000 yrs/10,000 yrs).

Results

Simulations

Our simulations demonstrate several potential features of the forest responses to Holocene climate variability, which would develop from the interaction of species' climate niches and a climate history including Holocene-length (orbitally forced) trends, additional millennial and centennial fluctuations, and decadal variability (Fig. 3). In the simulations, each pseudo-species has a fixed (deterministic) response to the synthetic climate history based on its sine-form response with taxon A dominant at high 'climate' index values (green, Fig. 3A), taxon B at intermediate values (tan, Fig. 3B), and taxon C at low values (blue, Fig. 3C). The first experiment shows how climate niches, approximated by sine-form response curves, would cause each taxon to rise and fall in concert with the synthetic centennial-to-millennial fluctuations around a slowly rising 'climate' trend (Fig. 3D).

The long-term trend causes taxon C (blue) to dominate for the first two millennia, followed by taxon B (tan), and then finally, taxon A (green). These phases are bound by rapid transitions generated by the interactions between the steepest portions of the non-linear response curves (Fig. 3A-C) and the additional millennial 'climate' variability, which accelerates the long-term trend at ca. 6500 and 2500 years (black line, Fig. 3D). Additional millennial and centennial fluctuations in the abundance of the three taxa also interrupt, and at times reverse, the major vegetation phases. Notably, taxon A (green) briefly increases from ca. 6000-4500 years, well

before it becomes the dominant in the last 2500 years; it then declines and almost disappears from the simulated vegetation from ca. 4500-2500 years when taxon C (blue) returns after an absence from ca. 6000-4500 years (Fig. 3D). Consequently, each pseudo-species has a large decline between 6500-4000 years: taxon C (blue) at ca. 6500 years, taxon A (green) at ca. 4500 years, and then taxon B (tan) at ca. 4000 years (Fig. 3D).

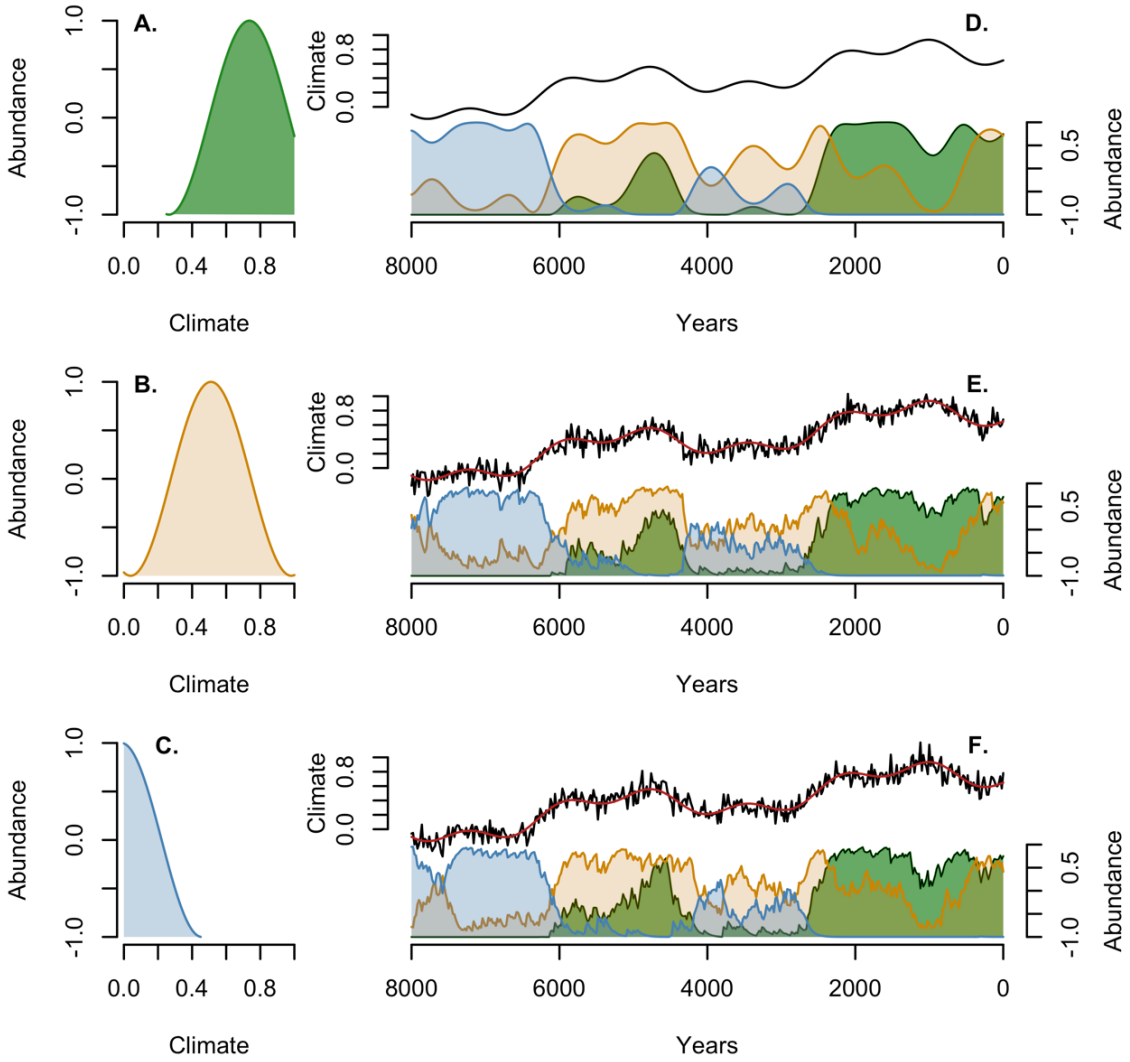

Figure 3. Simulations of the 8000-year histories of three pseudo-species (A-C) based on deterministic responses to synthetic climate histories (D-F), governed by their sine-form climate response curves (A-C). Black lines in D-F represent the 'climate' history used to drive each set of calculations; red lines in E-F show the trend and oscillations (same as in D) underlying the synthetic histories, which also include two different sets of stochastic decadal variability at the two different 'sites' represented in E and F. Colored shading shows outcomes from equations 1 and 2 for each pseudo-species: A (green), B (tan), and C (blue). Time progresses from 8000 years to year 0 to parallel the Holocene datasets.

281 The stochastic decadal 'climate' variability creates two additional effects (Fig. 3E-F). First,
282 abrupt changes replace the smoothly varying curves in the deterministic responses to the
283 synthetic 'climate' history. Both abrupt declines and increases, such as exist in many pollen
284 records (e.g., Schlenker et al. 2024), emerge when the steepest portions of the response curves
285 coincide with points where the added decadal variability accentuates the rates of 'climate'
286 change, such as when taxon B collapses rapidly at ca. 4500 years in the first of the two stochastic
287 experiments (tan, Fig. 3E). Second, the decadal variability differs between the two stochastic
288 experiments, just as it might at two different locations given the heterogeneity of short-term
289 climate variations, particularly regarding moisture and drought. Consequently, the timing of
290 abrupt changes, and even the presence (or not) of short-lived peaks in the abundance of the taxa,
291 differs between the two 'sites' represented by the two experiments (Fig. 3E-F).
292
293 A series of abrupt changes beginning at ca. 4500 years in the two experiments provide a useful
294 demonstration of the consequences of the deterministic response to the stochastic variability.
295 Taxon A (green), which had reached its early peak in abundance, declines abruptly – albeit
296 somewhat asynchronously – in the two experiments at ca. 4500 years (Fig. 3E-F). At the first
297 'site', taxon B (tan) declines abruptly and taxon C (blue) increases rapidly at the same time (Fig.
298 3E). However, at the second 'site', the asymptote of the response curve causes A (green) to
299 decline faster than the underlying centennial 'climate' change (red line in Fig. 3F), consistent
300 with some observations of vegetation changes leading their climatic driver (Williams et al. 2002,
301 Booth et al. 2012). The abrupt decline in B (tan) and increase in C (blue) then follows by several
302 centuries, creating a set of centennial-scale vegetation phases with A (green), B (tan), and then C
303 (blue) dominating in sequence (Fig. 3F). Subsequent centennial 'climate' oscillations repeat the

sequence of B and C peaks from ca. 4000-3000 years, although the character of the vegetation fluctuations differs between the 'sites' with taxon C (blue) rising abruptly twice, separated by a brief abrupt increase in A (green), at the second 'site' (Fig. 3F), but not at the first (Fig. 3E).

Three aspects of these simulations have direct relevance to the forest changes recorded by the pollen diagrams from Blanding Lake and Sunfish Pond:

1. Sequences of multiple abrupt tree declines (and increases), which bound centennial to millennial duration phases of dominance by different taxa;
2. Repetition of some short-lived phases, such as the multiple peaks in taxon C (blue) from ca. 4000-3000 years (Fig. 3E-F); and
3. Differences in the details among 'sites' (Fig. 3E-F), but consistent, underlying low-frequency fluctuations (Fig. 3D).

Sediment cores and chronologies

To evaluate these expectations and the history of the Tension Zone, sediment cores were collected from Blanding Lake and Sunfish Pond, which were 930 and 785 cm long respectively. Nine calibrated radiocarbon ages (Table 1) form the basis of the Blanding Lake chronology; a tenth date from the center of the core (>19,000 YBP) appears out of sequence (Fig. 4A). All ages derive from macroscopic charcoal. The bchron chronology provides regionally consistent ages of two widespread biostratigraphic features: 1) a peak in birch pollen percentages of >30% at 12,500 YBP (13,520-10,900 YBP, 95% C.I.), which is widely documented (Gaudreau and Webb 1985, Mayle et al. 1993) and typically dates to 13,000-12,500 YBP (Shuman et al. 2009), and 2) the mid-point of the mid-Holocene hemlock decline from 27 to 8% at 5050 YBP (5640-4950

327 YBP, 95% C.I.), which compares well with regional age estimates of 5280±180 YBP (Shuman et
328 al. 2009), and 5025 YBP (5160–4895 YBP, 95% C.I., Booth et al. 2012).

329

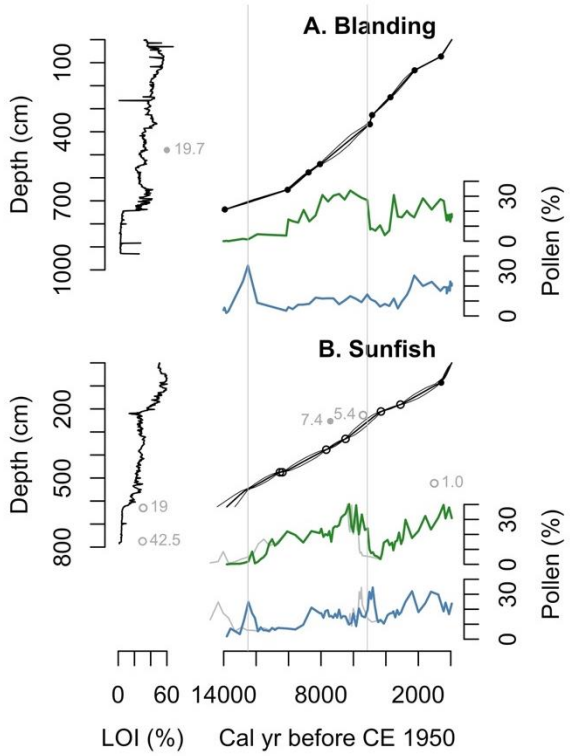

*Figure 4. Age-depth relationships, calibrated radiocarbon dates, loss-on-ignition (LOI) profiles by depth in core, and hemlock (**green**) and birch (**blue**) pollen percentages by age for A) Blanding Lake and B) Sunfish Pond. Closed circles indicate radiocarbon ages based on charcoal; open circles indicate ages derived from bulk sediment. Gray symbols indicate rejected ages, and gray hemlock and birch pollen percentage lines represent the chronology with rejected ages included. Vertical lines mark the Younger Dryas-aged birch peak and the mid-Holocene hemlock decline. Black lines show the median and 95% range of sample ages estimated using bchron.*

331 The Sunfish Pond chronology has several complications. Six calibrated radiocarbon ages were
332 accepted for the final bchron chronology (Fig. 4B), but five additional ages were rejected either
333 because they were out of stratigraphic position or because they created old, regionally
334 inconsistent ages for the late-Pleistocene birch peak (blue lines, Fig. 4) and the mid-Holocene
335 hemlock decline (green lines, Fig. 4). All but one of the accepted ages derive from bulk
336 sediment; the youngest age derives from macroscopic charcoal. The rejected ages have the same
337 mix of bulk sediment (4) and charcoal (1) ages. The final chronology included assigning the age
338 of the early birch peak from Blanding Lake in place of the oldest radiocarbon ages because these
339 two bulk ages of 19,100 and 42,500 YBP derive from the inorganic portion of the core and
340 would cause the birch peak to have an unrealistically old age of ~14,000 YBP (Fig. 4B).

In the mid-Holocene, a bulk sediment age of 5400 YBP was also rejected (Fig. 4B) because it caused the hemlock decline to have an age of >5700 YBP, which is >500 years older than the decline at nearly all sites in the northeast U.S. (Shuman et al. 2009, Booth et al. 2012). The 5400 YBP age derives from a sandy interval of the core and could include re-worked material. An adjacent 7400 YBP charcoal age also appears to indicate the presence of some old carbon; removing these ages places the hemlock decline at 5070 YBP (5960-4490 YBP, 95% C.I.)

Pollen stratigraphies

The Blanding Lake and Sunfish Pond pollen stratigraphies track patterns of vegetation change consistent with those expected in the region (Watts 1979, Barnosky et al. 1988, Oswald et al. 2007). At both lakes, conifers dominate the earliest portion of the record (Fig. 5-6), including in association with 1) the regionally recognizable birch peak during the Younger Dryas (YD) chronozone (Gaudreau and Webb 1985, Barnosky et al. 1988, Peteet et al. 1990, Mayle et al. 1993) and 2) the subsequent phase when white pine (*P. strobus*) increased to >40%, which is also typical of the early Holocene in the region (Watts 1979, Shuman et al. 2009).

After ca. 10,000 YBP, different combinations of four major taxa, birch, beech, hemlock, and oak, dominate the pollen records along with important pulses of white pine, hickory, and chestnut (Fig. 5-6). During the mid-to-late Holocene (5000-2500 YBP), sequences of short-lived (millennial-to-centennial) phases of unique composition developed, beginning with the hemlock decline. These include maxima in the percentages of beech (>30%), oak (>35%), and then white pine pollen (>15%) as well as in minor types such as sugar maple (4-7%), ironwood (3-4%) and

chestnut (2-5%). However, chestnut, birch, hemlock, and diploxylon pines (*P. banksansia, P. resinosa, and P. rigida*) are all modestly more abundant at Sunfish Pond than Blanding Lake. Likewise, pollen types representative of European land clearance (*Ambrosia, Rumex*, and Poaceae) appear in the upper 50 cm at Blanding Lake (Fig. 5), but are not important at Sunfish Pond where historic land clearance was limited (Fig. 6).

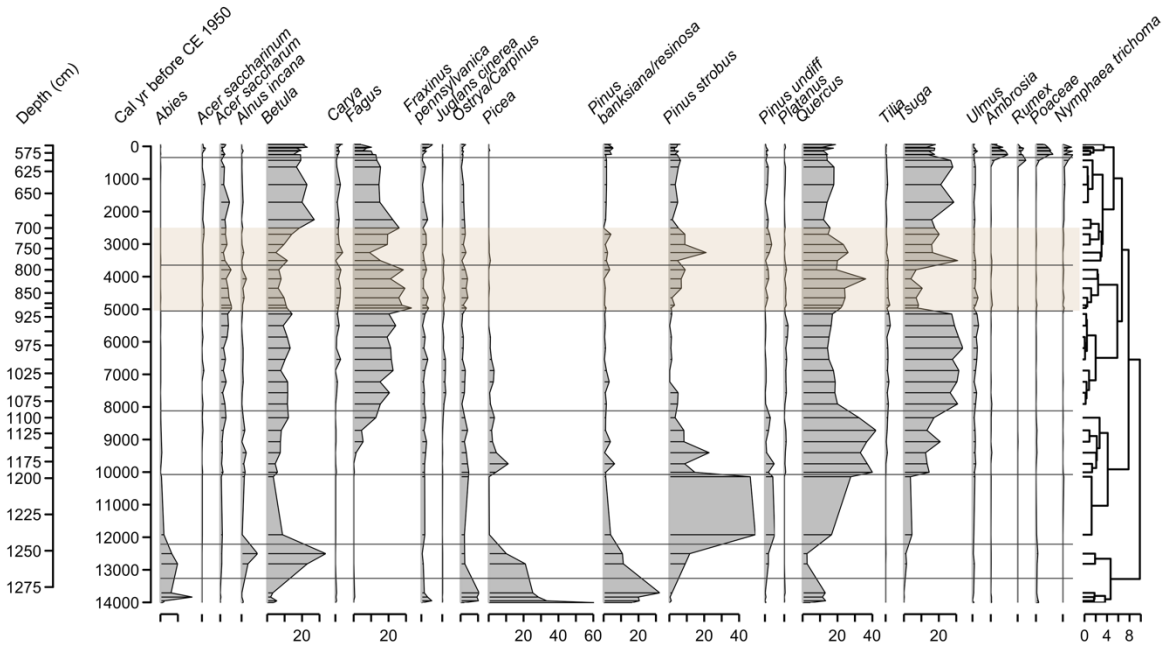

Figure 5. Summary pollen percentages from Blanding Lake. Horizontal lines represent the significant breaks (zones) based on the Bray-Curtis CONISS clustering at right. Tan shading highlights the interval from 5000-2500 YBP. Depths represent depth below the water surface. Taxa shown have a total sum of percentages across all samples that exceeds 20%.

Mid-Holocene variability: Blanding Lake

Beginning with the hemlock decline, the mid-Holocene pollen stratigraphy from Blanding Lake includes three millennial-scale phases or pollen zones with distinctly different composition, defined by maxima in the abundances of different taxa (Fig. 5):

- 5050-3650 YBP (910-790 cm): During the period of minimum hemlock percentages, oak returns to near its early Holocene abundance (>35%) as beech (>30%), sugar maple (4-7%), and ironwood (3-4%) reach their maxima.

- 3650-3140 YBP (790-750 cm): The recovery of hemlock coincides with a notable minimum in beech (<15%) and a sequence of peaks in hemlock (>30% at 3510 YBP), white pine (>20% at 3260 YBP), and oak pollen percentages (>25% at 3250-3010 YBP).
- 3140-1980 YBP (750-670 cm): The mid-Holocene oak and pine peaks end as their pollen percentages decline from 23-12% and 9-2% respectively. Beech and hemlock pollen percentages exceed 20% as birch pollen percentages progressively rise to >25%.

The resolution of the Blanding Lake record is insufficient to substantiate the details of the centennial (300-500 yr) variations in the mid-Holocene, but the variations include two distinct peaks in oak at 4070 YBP and then again at 3250-3010 YBP (Fig. 5).

Mid-Holocene variability: Sunfish Pond

At Sunfish Pond, the mid-Holocene also contains a series of distinct phases or pollen zones following the hemlock decline (Fig. 6):

- 5070-4620 YBP (837-812 cm) – After hemlock declines abruptly, both beech and birch reach their peak pollen percentages (28-35%). White pine and chestnut pollen percentages, which had briefly risen to >5% and 2% respectively before 5070 YBP, also decline to near-zero minima in the same samples as the hemlock decline.
- 4620-4288 YBP (812-796 cm) – Here, beech and birch pollen percentages decline rapidly, but oak pollen percentages peak at 30-32% and white pine and chestnut pollen percentages recover to >10% and 2%. Hickory pollen percentages also achieve their maximum (>4%).
- 4288-2870 YBP (796-758 cm) – White pine pollen percentages continue the progression of mid-Holocene peaks, rising to >20% at the base of this zone as hemlock pollen

percentages also rise sharply again to 15%. Peak chestnut pollen percentages (5%) help to define the top of the zone.

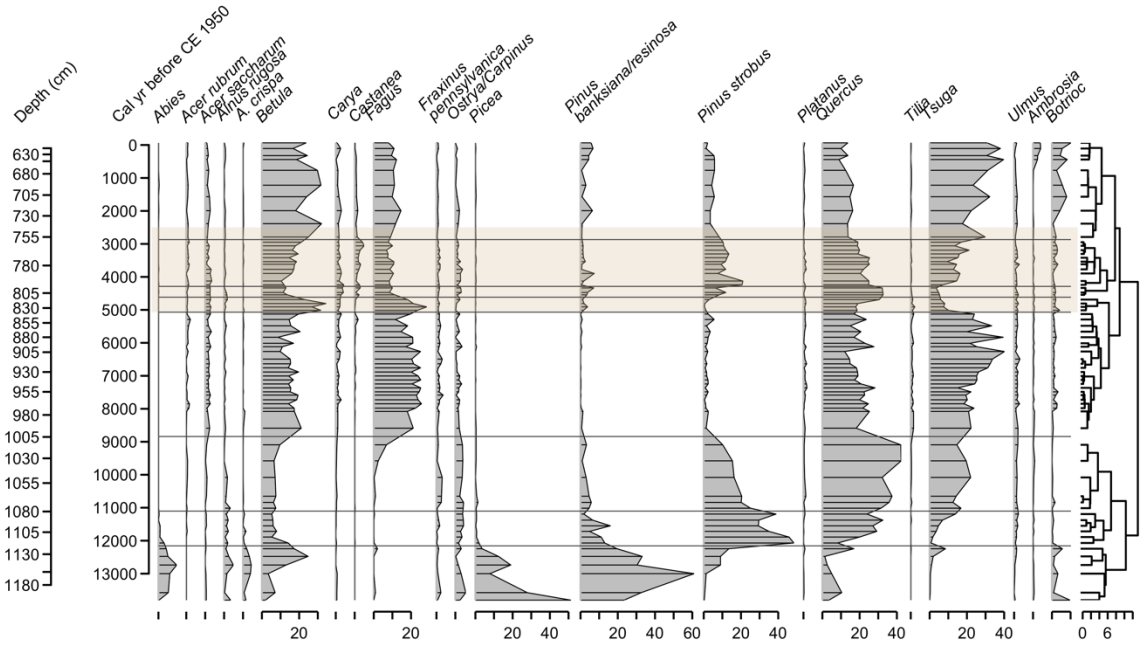

Figure 6. Summary pollen percentages for Sunfish Pond. Horizontal lines represent the significant breaks (zones) based on the Bray-Curtis CONISS clustering at right. Tan shading highlights the interval from 5000-2500 YBP. Taxa shown have a total sum of percentages across all samples that exceeds 20%.

The details of the Sunfish Pond stratigraphy highlight a series of abrupt tree declines. After hemlock declined abruptly at 5070 YBP, birch and beech both declined rapidly at 4800 YBP followed by oak and hickory at 4250 YBP, white pine at 4000 YBP, and chestnut at 2800 YBP (Fig. 7). The changes also include both low-frequency, millennial-scale maxima and multi-century peaks that depart from the slow trends. Low-frequency maxima represented by loess smoothers include a double-peaked maximum in oak (4810-3300 YBP) and individual maxima in hickory (4910-3300 YBP), ironwood (4470-3420 YBP), and white pine and chestnut (4690-2790 YBP). The additional superimposed multi-century peaks include five distinct phases (Fig. 7): 1) birch and beech (5100-4800 YBP), 2) oak, hickory, and chestnut (4800-4250 YBP), 3)

white pine, hemlock, and ironwood (4250-3800 YBP), 4) oak and white pine (3800-3200 YBP), and 5) chestnut (3200-2800 YBP).

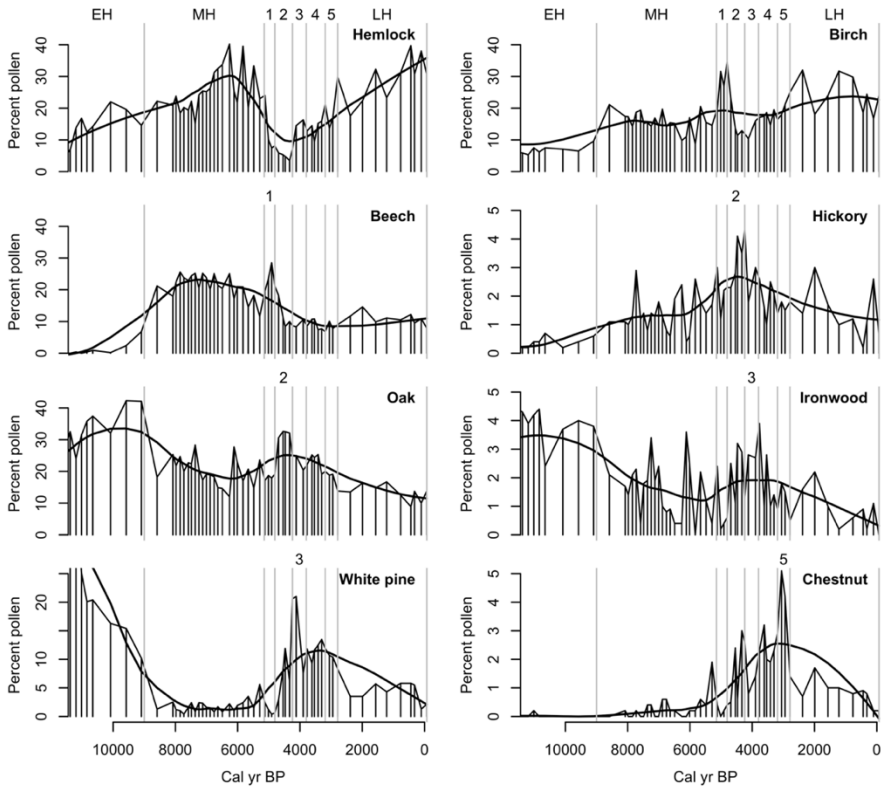

Figure 7. Sunfish Pond pollen percentages plotted by time. Loess smoothers (thick black lines) were fit with 5000-yr spans. Vertical gray lines mark 11700, 9000, 5150, 4810, 4240, 3800, 3190, and 2790 YBP, and divide the early Holocene (EH), mid Holocene before the hemlock decline (MH), the late Holocene (LH), and the five phases containing different peaks in pollen percentages of important tree taxa.

Discussion

The forest changes recorded at the two lakes include three timescales of variation (Fig. 4-6) like those generated by our heuristic simulations of forest responses to Holocene climate changes (Fig. 3). The two records include the classic sequence of long-term vegetation trends and pollen zones consistent with the slowly varying aspects of the regional climate (Deevey 1943, Davis 1969, Watts 1979, Shuman et al. 2004)(Fig. 5-6). However, they also include additional millennial fluctuations (Fig. 7, smooth lines), superimposed centennial maxima, and abrupt declines and increases (Fig. 7, raw data). Blanding Lake is representative of many records in the region with poorly resolved hints of the centennial variations, but when resolved at ~100-yr sample spacing, the sequence of events at Sunfish Pond is like that at other northeastern highland

and Tension Zone sites, such as Guilder and Little ponds, Massachusetts (Oswald et al. 2018) and Balsam and Ballston lakes, New York (Ibe 1985, Toney et al. 2003)(Fig. 1).

Potential processes and triggers

Previously, mid-Holocene forest phases in northeastern forests have been attributed to the removal of hemlock by a pathogen (e.g., Fuller 1998), but the assumptions used to infer a pathogen outbreak (by Davis 1981) no longer hold (Foster et al. 2006, Shuman et al. 2023; see more below). Even studies that emphasize biotic drivers of the decline point to climate for sustaining >1500 years of low hemlock abundance (Fuller 1998, Booth et al. 2012). Consequently, assuming that the forest dynamics here are simply a response to hemlock's demise takes for granted that hemlock declined for a species-specific reason ("begs the question"). However, the subsequent centennial forest phases may represent several intrinsic dynamics: 1) competitive release and resulting successional dynamics following the hemlock decline or other disturbances; 2) state-shifts triggered by repeated (compounded) disturbances (Turner et al. 1993, Paine et al. 1998); or 3) population variations shaped by the contingency of extreme events and autoregressive population processes (Jackson et al. 2009, Ramiadantsoa et al. 2019).

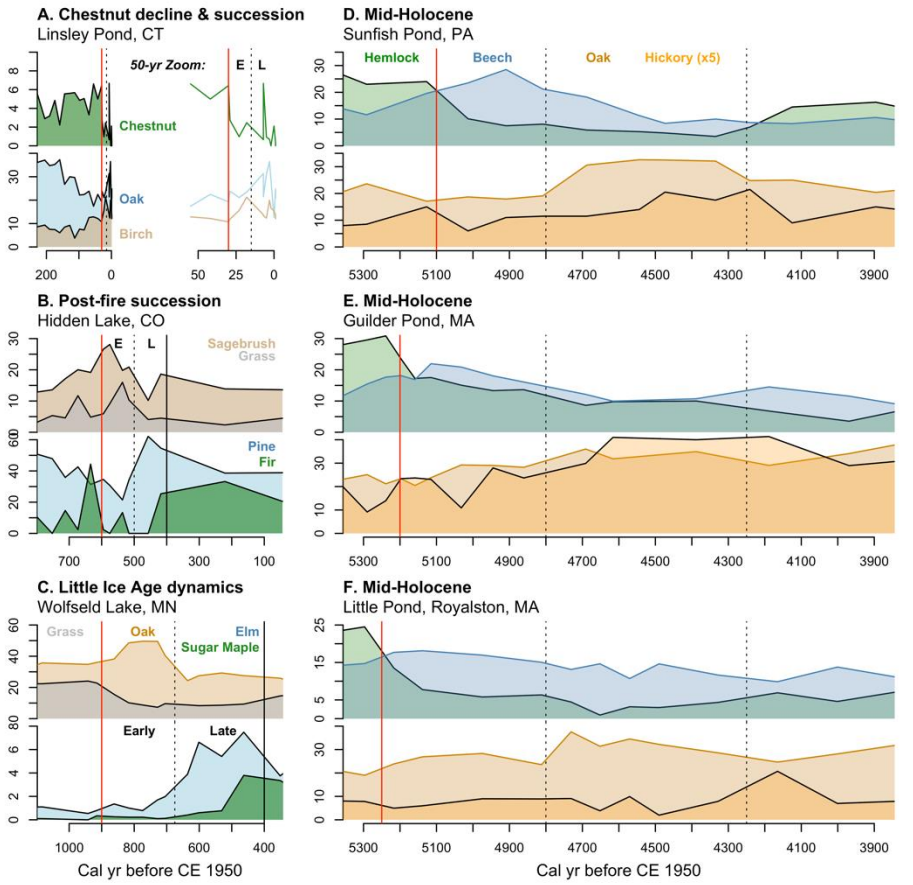

Figure 8. Fossil pollen records of known examples of successional dynamics (A-C) compared to mid-Holocene changes at (D) Sunfish Pond, PA, and (E,F) comparator 'Tension Zone' lakes (Guilder and Little ponds, MA)(Oswald et al., 2018). Red vertical lines show the timing of disturbances or the first change in the series shown. Dashed lines mark the onset of subsequent vegetation phases, which are labelled as representing early ("E") or late ("L") successional phases in A-C. Unfilled line graphs in A zoom in on the details of the last 50 years there. All other time scales are the same showing 600 years in A-C and 1400 years in D-F.

Competitive release and succession – Hemlock's removal from the forest could have released other taxa from competition for habitat and canopy space. For example, beech is an excellent gap-colonizer (Canham 1990, Poage and Peart 1993) and is often co-dominant with hemlock at the landscape scale (Fig. 1)(Cogbill et al. 2002). Consequently, beech could have had both an immediate and long-term competitive advantage after the hemlock decline (Fuller 1998). However, the various mid-Holocene mixtures of taxa do not wholly depend upon the decline and recovery of hemlock (Fig. 4-6). For example, white pine, oak, and chestnut became important for a millennium in the mid-Holocene at Blanding and Sunfish, but did not increase until after hemlock began its recovery (Fig. 7). At other sites across the Tension Zone region, increases in

taxa like oak and pine sometimes began before the hemlock decline (Mott and Farley-Gill 1978) or even developed in the absence of abundant hemlock (Gilliam et al. 1967, Tzedakis 1992).

Three examples of succession recorded by pollen records demonstrate responses to disturbance and climate change at landscape and larger scales (Fig. 8). However, these examples show unidirectional trajectories of seral stages over 25-250 years (Fig. 8), which differ in duration and progression from the repeated peaks and declines of the taxa near the Tension Zone (Fig. 7):

1. **Succession following the removal of a single canopy species (Fig. 8A)** – At Linsley Pond, Connecticut, the early-20th century chestnut blight caused a sharp decline in chestnut pollen percentages (red line, Fig. 8A)(Brugam 1978); Davis (1981) cited the example of the blight in making the case that the hemlock decline may have been driven by a similar disease. However, within 15 years of the blight, birch pollen percentages peaked, representing the early successional response ("E" in the 50-yr zoomed diagram, Fig. 8A). Within 30 years, oak pollen percentages had risen to replace both birch and chestnut during the late ("L") successional response. The sequence demonstrates that the successional responses to the rapid removal of a single key taxon would have played out far more rapidly than could be detected in the Sunfish Pond data and would not suitably explain centennial vegetation phases after the hemlock decline (Fig. 8D-F).
2. **Succession following high-severity, stand-replacing fire (Fig. 8B)** – At Hidden Lake, Colorado, pollen percentages illustrate the timescale of succession following high severity disturbance that removed much of the forest canopy (Calder et al. 2019). A large charcoal layer indicates a wildfire or series of fires at ca. 600 YBP (red line, Fig. 8B).

After the fire, pollen percentages of trees declined and shrub or herbaceous taxa such as sagebrush (*Artemisia*) and grass (Poaceae) increased to >50% ("E" in Fig. 8B), which is unusual for a forested setting but consistent with a post-fire meadow. After ~100 years, pine pollen percentages began increasing again, revealing post-fire lodgepole pine recovery, but by ~200 years after the fire, pine pollen percentages had peaked and declined as shade-tolerant, late-successional taxa, such as fir (*Abies*), increased ("L" in Fig. 8B). The 200-yr progression of phases involves the complete re-establishment of forest over a sufficiently large fraction of the pollen source area to be detectable here. However, the full progression is shorter than the 300-500 year duration of individual phases, such as the first beech-birch peak, at the Tension Zone sites (Fig. 8D-F).

3. **Open woodland to deciduous forest transition during the Little Ice Age (Fig. 8C)** – In the Big Woods region of Minnesota, climate changes and a regional reduction in wildfire favored a transition from open oak woodlands to temperate deciduous forest (Grimm 1983). Forest landscape simulations confirm that successional dynamics, including significant seed dispersal required to spread new trees across a large landscape, could explain the resulting sequence of changes (Berland et al. 2011). At first, the changes favored an increase in oak, replacing grass and other herbaceous taxa (the "Early" phase in Fig. 8C). Then, shade-tolerant taxa, such as elm and sugar maple, increased at the expense of oak (the "Late" phase in Fig. 8C). The changes were likely asynchronous across the pollen source area, which caused the successional trends to persist longer than within individual stands (e.g., Bormann and Likens 1994) or than after widely synchronized disturbances (Fig. 8A-B). The climate change may have extended the duration of each phase to 200-300 years (Fig. 8C). Simulations indicate, however,

that such a climatic effect is not required; the duration is largely successional (Berland et al. 2011). Asynchronous succession over large portions of a pollen source area can produce a slow, century-scale (although not multi-millennial) progression of taxa (Davis and Botkin 1985, Campbell and McAndrews 1993, Berland et al. 2011).

Unlike these examples, the tree sequences after the hemlock decline do not represent any obvious seral pattern or single progressive trajectory. Hemlock itself has brief periods of abundance and then secondary declines (at 3510 YBP at Blanding Lake and 4250-3800 YBP at Sunfish Pond) rather than a progressive return to a pre-disturbance state. Asynchrony of these secondary changes, and of the classic hemlock decline (red vertical lines, Fig. 8D-F), is comparable to the deterministic differences in the specific timing of abrupt changes among 'sites' in our simulation experiments (e.g., different timing of the abrupt declines of pseudo-species A, green, and B, tan, at ca. 5000-4000 years in the simulations, Fig. 3E-F).

Compound disturbances, contingency effects, and population dynamics – State shifts in forest composition can also emerge after multiple, repeated ("compound") disturbances with some species surviving an initial disturbance only to be killed by a second disturbance (Turner et al. 2019). Historical contingencies, i.e., the sequence of events, could influence how species to respond to subsequent changes (Jackson et al. 2009). Population processes alone may also produce abrupt declines in the abundance of major tree taxa (Ramiadantsoa et al. 2019). However, the effects of disturbance and contingencies, if not population dynamics, would be highly localized because disturbances like storms, wildfires, and drought tend to have small or heterogeneous spatial extents (e.g., Turner et al. 1998, Pederson et al. 2014). Even the impacts of

579 extremely large wildfire events appear as secondary features superimposed on close climate-
580 pollen relationships in other settings (Calder and Shuman 2017). They are more likely to impact
581 individual forest stands than whole regions. By contrast, the initial rise and then decline of beech,
582 oak, hickory, and pine played out similarly at multiple sites in different highland areas (Fig. 8D-
583 F), which are unlikely to have been impacted by the same extreme events or population
584 dynamics. Similar phases also affected other Tension Zone sites in Massachusetts (Fig. 8), New
585 York (Ibe 1985, Toney et al. 2003), and Ontario (Bennett 1986, Fuller 1998). Such processes not
586 only would have to explain these widespread decreases in beech and increased in oak near the
587 Tension Zone, but should also predict the reverse patterns of change (beech increase and oak
588 decrease) in coastal areas (Foster et al. 2006). Climate variations could, by contrast, predict such
589 patterning (Marsicek et al. 2013, Shuman et al. 2023).
590
591 *Similarities between the simulations and stratigraphies*
592 Many aspects of the Blanding Lake and Sunfish Pond pollen records have precedents in our
593 simulations (Fig. 3). The simulations demonstrate that the sequences of abrupt declines do not
594 necessarily require disturbances as triggers and that stochastic contingency could be limited to its
595 role in short-term climate variability (Fig. 3). The hemlock decline has a parallel in the abrupt
596 decline and then recovery of pseudo-species A (green in Fig. 3D-F). Likewise, the model reveals
597 how differences in the climate niches (Fig. 3A-C) can create asynchrony in the declines of
598 multiple taxa even when they represent responses to the same millennial or centennial climate
599 oscillation (Fig. 3D). For example, the peaks and rapid declines of birch and beech, which
600 followed the hemlock decline by ~300 years at Sunfish Pond (Fig. 4-6), represent a dynamic like
601 the simulated sequence of declines in pseudo-species A (green) and then B (tan) several centuries

602 later (Fig. 3F). Finally, the northward expansion of oak and white pine after the hemlock, beech,
603 and birch declines (Fig. 4-6) appears analogous to the simulated renewal and multiple subsequent
604 peaks in the abundance of pseudo-species C (blue in Fig. 3D-F). In the model, the changes
605 developed in response to a combination of millennial and centennial climate variations, like
606 those reconstructed in the regional temperature gradients (Fig. 9A) and moisture availability
607 (Fig. 9B).

608

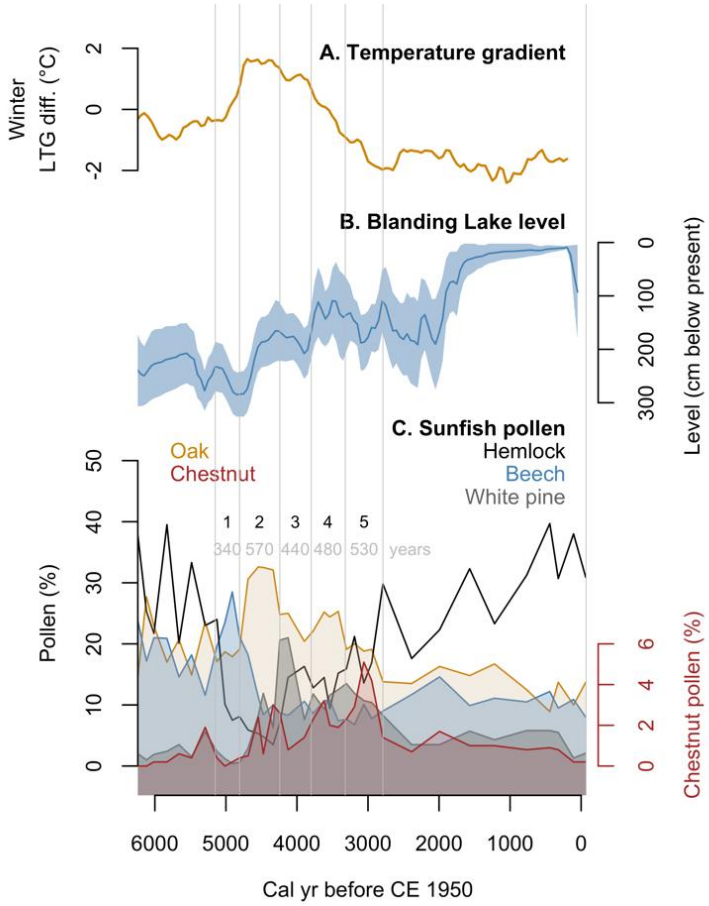

Figure 9. A) Differences in the steepness of the north-south (latitudinal) temperature gradient (LTG diff.) across the region, which warms Pennsylvania when positive (Shuman et al., 2023), and B) the history of water-level changes from Blanding Lake (Shuman and Burrell, 2017) provide context for C) the different phases of the pollen record from Sunfish Pond over the past 6000 years. Vertical lines, numbered 1-5, mark the centennial-scale vegetation phases (shown in Fig. 7), which may correspond in time with water-level fluctuations (B) and with other centennial climate variations in the region (Fig. 1C).

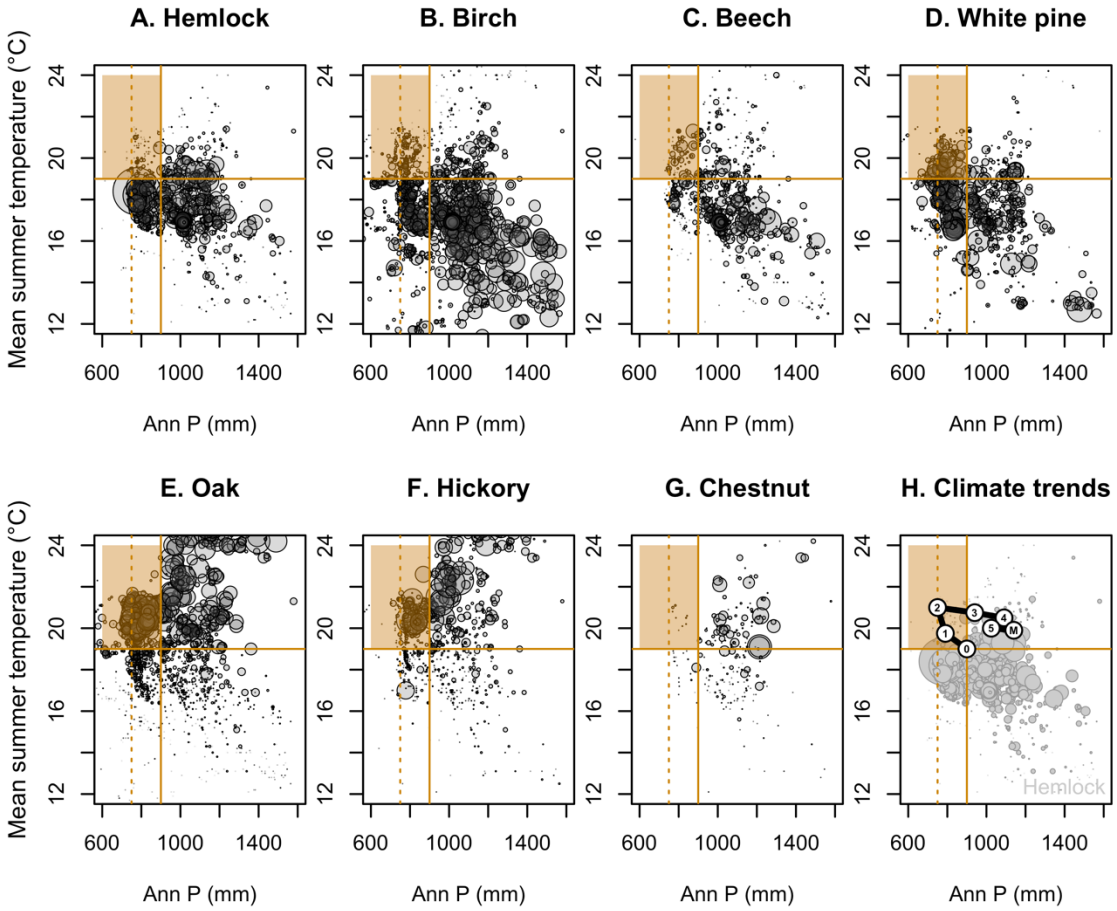

630

631 *Figure 10. Modern pollen-climate relationships from North America east of 100°W longitude and north*
632 *of 35°N latitude. Points show the relative abundances of hemlock (A), birch (B), beech (C), white pine*
633 *(D), oak (E), hickory (F), and chestnut (G) pollen with respect to mean summer (June-August)*
634 *temperatures and mean annual precipitation ("Ann P"). Plausible climate trends (H) link the period*
635 *before the hemlock decline (0) with each of the post-decline vegetation phases (1-5 in Fig. 7 & 9C) and*
636 *modern ("M"); the trends include millennial warmth combined with long-term moistening and centennial*
637 *droughts (Fig. 9A-B). Orange lines mark mean summer temperatures of 19°C (horizontal solid line) and*
638 *annual precipitation equal to 900 mm (vertical solid line) and 750 mm (vertical dashed line); orange*
639 *shading marks wetter and warmer climates than the solid line thresholds where hemlock is absent, but not*
640 *other taxa like beech. Circle sizes are scaled to abundance in each sample; oak and birch symbols are*
641 *scaled to one-third the size of hemlock, beech, and white pine and one-sixth the size of hickory and*
642 *chestnut to account for differences in total abundance.*

643

Comparing the climate history to the climate niches of the key taxa

Holocene climate variations, including temperature and precipitation changes at millennial and centennial scales (Fig. 9A-B), may have provided the pacing and regional patterning to generate the observed sequence of centennial-scale phases of community composition (Fig. 9C). Davis (1981) initially ruled out climate as a driver of the hemlock decline because evidence did not exist for millennial and centennial scale variability or abrupt mid-Holocene climate changes, but that is no longer the case (Fig. 9A-B)(e.g., Willard et al. 2005, Menking et al. 2012, Shuman and Burrell 2017, Shuman et al. 2023). In Pennsylvania, the association between climate and forest variability (Fig. 9) does not differ substantially from that in our simulations (Fig. 3). The trajectory of the climate moved through the climate niches of the different taxa (Fig. 10), increasing and decreasing them sequentially as expected by our simulations (Fig. 3).

As in the simulations, the different taxa at Blanding Lake and Sunfish Pond have differences in their climate niches that help to explain the forest histories (Fig. 10). For example, from >8000 to 5000 YBP, the regional climate shifted from cooler than 19°C and drier than 900 mm (intersection of solid orange lines in each panel, Fig. 10) to a warmer and drier climate (upper left shaded area in each panel of Fig. 10). The niches represented by modern pollen-climate relationships indicate that hemlock, but not beech and birch, would have declined once summer temperatures exceeded 19°C and precipitation fell below 900 mm (upper left quadrants, shading, Fig. 10); similar climates exist today in parts of southern Michigan, Ohio, and western New York where hemlock is rare (Thompson et al. 1999, Williams et al. 2006). Later climate changes produced a warm and wet climate (upper right quadrants, Fig. 10), favoring oak and hickory over beech, which would have then declined. As the region ultimately cooled and moistened toward

667 present (lower right quadrants, Fig. 10), other taxa like white pine (Fig. 10D) and chestnut (Fig.
668 10G) would have increased.
669
670 *Ecotone changes*
671 The interaction among climate changes and different niches explains why the sequence of forest
672 phases dominated by 1) hemlock-beech-birch, 2) oak-hickory, 3) white pine, and eventually 4)
673 renewed hemlock-beech-birch forests (Fig. 5-6) has a spatial analogy in 18th century forests (Fig.
674 1)(Cogbill et al. 2002, Thompson et al. 2013). Walther's Law states that stratigraphically
675 adjacent paleoenvironments typically have equivalents in spatially-adjacent environments today
676 (Middleton 1973). It applies well to the forest sequences. Cold-hardy, mesic hemlock-beech-
677 birch forests grew north of the ecotone at the time of European colonization (green, yellow, Fig.
678 1). To the south, a narrow band of white pine forests helped to define the 18th century ecotone
679 (blue, Fig. 1); oak-dominated forests extended southward from there (tan, Fig. 1). With mid-
680 Holocene warming (Fig. 9A), the ecotone passed northward after ca. 5000-4800 YBP as oak
681 populations expanded (orange, Fig. 9C) and replaced hardwood stands around Sunfish Pond
682 (blue and black, Fig. 9C). Oak abundance locally became equivalent to southern sites such as
683 Tannersville Swamp (Fig. 1)(Watts 1979). With cooling after ca. 4500 YBP, the ecotone again
684 shifted southward: the pine belt (gray, Fig. 9C) and then renewed hardwoods replaced the mid-
685 Holocene oak forests (blue and black versus orange, Fig. 9C).
686
687 An ecologically-significant Holocene moistening trend (Fig. 9B)(Shuman et al. 2019) further
688 modified the spatial patterns of change. The long-term increase in precipitation recorded by
689 rising lake levels (Fig. 9B) created a general westward shift in ecoclimatic conditions; after ca.

4500 YBP, the dry early-to-mid-Holocene climate with <1000 mm of annual precipitation shifted westward out of Pennsylvania into the Ohio River Valley and surrounding regions where such conditions exist today. Thus, the beech-dominated phase at Sunfish Pond from 5000-4800 YBP and the subsequent oak-hickory peak from 4800-4250 YBP have similarities to historic forests in the warm, dry climate of western New York, Ohio, Indiana and Michigan (Paciorek et al. 2016). As moisture increased, such forests shifted westward. Oak and hickory declined and were not followed by a full recovery of the earlier beech-dominated communities at Sunfish Pond (blue, Fig. 9C). They were replaced locally, instead, by chestnut-white pine communities (red and gray, Fig. 9; in the upper right warm/wet quadrants of Fig. 10) until regional cooling also shifted these communities to their 18th century locations south of Sunfish Pond and Blanding Lake (blue, Fig. 1).

Conclusions

Appalachian forests, such as those around Blanding Lake and Sunfish Pond, never achieved persistent steady states. Novel communities repeatedly developed and then dissipated within 300-500 years. Some (e.g., oak-hickory-chestnut phases) formed and reformed, but others (e.g., the beech-birch phase at Sunfish Pond) formed only once. The changes encompass both the hemlock decline and the regional arrival of chestnut, but the landscape-scale changes and the extensive communities that they produced did not appear to represent seral sequences (Fig. 8) or progressive trajectories contingent on a “ratchetting” sequence of droughts or population dynamics (Paine et al. 1998, Jackson et al. 2009). Instead, even seemingly stochastic differences among sites (e.g., Fig. 3E-F) can be parsimoniously explained as part of large spatial dynamics coordinated by the full spectrum of multi-variate climate variation (Fig. 10). The patterns of

change in the forest histories (Fig. 7 & 9) do not differ meaningfully from the types of abrupt changes, fluctuations, and short-lived phases generated by a simple deterministic response to a variable climate (Fig. 3). Even though the fine spatial details of such changes at stand scales are stochastic and not strongly deterministic, their emergent outcomes at large scales do not appear to differ dramatically from deterministic expectations (Webb 1986, Shuman et al. 2019).

Small differences in species' climate relationships can explain the individualistic responses of the key tree taxa to the climate changes. Consequently, both climate history and the climate niches of the different taxa could be better studied, along with direct evidence of forest disturbances and plant physiological responses to shifting climates, to help explain the past and anticipate the future; e.g., just because both hemlock and beech are 'mesic' taxa did not mean that they responded to mid-Holocene climatic variability in the same way (compare their presence in the orange shaded region of Fig. 10). The resulting novel forest communities, and episodes of turnover between them, likely developed rapidly as the different taxa with different climatic preferences responded to the novel combinations of seasonal temperatures and precipitation (Fig. 9-10). If so, vegetation at landscape and larger scales is highly sensitive to climate changes, which will undoubtedly yield complex, rapid forest changes again today.

Acknowledgements

We thank J. Williams, D. Foster, and W. Oswald for useful comments on the manuscript. Funding was provided by the Roy J. Shlemon Center for Quaternary Studies at the University of Wyoming and NSF Division of Environmental Biology.

References

Allison, T.D., Moeller, R.E. & Davis, M.B. (1986) Pollen in laminated sediments provides evidence for a mid-Holocene forest path ogen outbreak. Ecology 67, 1101–1105.

Anderson, R.S., Davis, R.B., Miller, N.G. & Stuckenrath, R. (1986) History of late- and post-glacial vegetation and disturbance around Upper South Branch Pond, northern Maine. Canadian Journal of Botany 64, 1977–1986.

Baker, W.L. (1989) Landscape Ecology and Nature Reserve Design in the Boundary Waters Canoe Area, Minnesota. Ecology 70, 23–35.

Barnosky, A.D., Barnosky, C.W., Nickmann, R.J., Ashworth, A.C., Schwert, D.P. & Lantz, S.W. (1988) Late Quaternary Paleoecology at the Newton Site, Bradford Co., Northeastern Pennsylvania: Mammuthus Columbi, Palynology, and Fossil Insects. Bulletin of the Buffalo Society of Natural Sciences 33, 173–184.

Bennett, K.D. (1986) Holocene history of forest trees in southern Ontario. Can. J. Bot 65, 1792–1801.

Berg, T.M., Edmunds, W.E. & Geyer, A.R. (1980) Geologic map of Pennsylvania (2nd edition), scale 1:250,000. Pennsylvania Geological Survey.

Berland, A., Shuman, B. & Manson, S. (2011) Simulated Importance of Dispersal, Disturbance, and Landscape History in Long-Term Ecosystem Change in the Big Woods of Minnesota. Ecosystems 14, 398–414. https://doi.org/10.1007/s10021-011-9418-x

Bhiry, N. & Filion, L. (1996) Mid-Holocene hemlock decline in eastern North America linked with phytophagous insect activity. Quaternary Research 45, 312.

Booth, R.K., Brewer, S., Blaauw, M., Minckley, T.A. & Jackson, S.T. (2012) Decomposing the mid-Holocene Tsuga decline in eastern North America. Ecology 93, 1841–1852. https://doi.org/10.1890/11-2062.1

Bormann, F.H. & Likens, G.E. (1994) Pattern and process in a forested ecosystem : disturbance, development, and the steady state based on the Hubbard Brook ecosystem study. ed. byAnonymous,. Springer-Verlag, New York.

Braun, D.D. (2011) Chapter 40 - The Glaciation of Pennsylvania, USA. In: Developments in Quaternary Sciences. (ed. by J. Ehlers, P.L. Gibbard, and P.D. Hughes), Quaternary Glaciations - Extent and Chronology., pp. 521–529, Elsevier. https://doi.org/10.1016/B978-0-444-53447-7.00040-4

Brugam, R.B. (1978) Pollen indicators of land-use change in southern Connecticut. Quaternary Research 9, 349–362.

768 Calder, W.J. & Shuman, B. (2017) Extensive wildfires, climate change, and an abrupt state
769 change in subalpine ribbon forests, Colorado. Ecology 98, 2585–2600.
770 https://doi.org/10.1002/ecy.1959

771 Calder, W.J., Stefanova, I. & Shuman, B. (2019) Climate–fire–vegetation interactions and the
772 rise of novel landscape patterns in subalpine ecosystems, Colorado. Journal of Ecology
773 107, 1689–1703. https://doi.org/10.1111/1365-2745.13138

774 Campbell, I.D. & McAndrews, J.H. (1993) Forest disequilibrium caused by rapid Little Ice Age
775 cooling. Nature 366, 336–338. https://doi.org/10.1038/366336a0

776 Canham, C.D. (1990) Suppression and Release During Canopy Recruitment in Fagus
777 grandifolia. Bulletin of the Torrey Botanical Club 117, 1–7.
778 https://doi.org/10.2307/2997123

779 Clifford, M.J. & Booth, R.K. (2015) Late-Holocene drought and fire drove a widespread change
780 in forest community composition in eastern North America. The Holocene 25, 1102–
781 1110. https://doi.org/10.1177/0959683615580182

782 Cogbill, C.V., Burk, J. & Motzkin, G. (2002) The forests of presettlement New England, USA:
783 spatial and compositional patterns based on town proprietor surveys. Journal of
784 Biogeography 29, 1279–1304. https://doi.org/10.1046/j.1365-2699.2002.00757.x

785 Davis, M.B. (1969) Climatic changes in southern Connecticut recorded by pollen deposition at
786 Rogers Lake. Ecology 50, 409–422.

787 Davis, M.B. (1981) Outbreaks of forest pathogens in Quaternary history. Proceedings of the
788 Fourth International Palynological Conference 3, 216–227.

789 Davis, M.B. & Botkin, D. (1985) Sensitivity of cool-temperate forests and their fossil pollen
790 record to rapid temperature change. Quaternary Research 23, 327–340.

791 Deevey, E.S. (1943) Additional pollen analyses from southern New England. American Journal
792 of Science 241, 717–752.

793 Faegri, K. & Iverson, J. (1989) Textbook of Pollen Analysis. ed. byAnonymous,. John Wiley and
794 Sons, New York.

795 Foster, D.R. & Boose, E.R. (1992) Patterns of forest damage resulting from catastophic wind in
796 central New England. Journal of Ecology 80, 79–98.

797 Foster, D.R., Clayden, S., Orwig, D.A., Hall, B. & Barry, S. (2002) Oak, chestnut and fire:
798 climatic and cultural controls of long-term forest dynamics in New England, USA.
799 Journal of Biogeography 29, 1359–1379.

800 Foster, D.R., Oswald, W.W., Faison, E.K., Doughty, E.D. & Hansen, B.C.S. (2006) A climatic
801 driver for abrupt mid-Holocene vegetation dynamics and the hemlock decline in New
802 England. Ecology 87, 2959–2966.

Foster, D.R. & Zebryk, T.M. (1993) Long-Term Vegetation Dynamics and Disturbance History of a Tsuga-Dominated Forest in New England. Ecology 74, 982–998.

Fuller, J.L. (1998) Ecological impact of the mid-Holocene hemlock decline in southern Ontario, Canada. Ecology 79, 2337–2351. https://doi.org/10.1890/0012-9658(1998)079[2337:EIOTMH]2.0.CO;2

Fuller, J.L., Foster, D.R., McLachlan, J.S. & Drake, N. (1998) Impact of Human Activity on Regional Forest Composition and Dynamics in Central New England. Ecosystems 1, 76–95.

Gaudreau, D. & Webb, T. (1985) Late-Quaternary pollen stratigraphy and isochrone maps for the northeastern United States. In: Pollen Records of Late-Quaternary North American Sediments. (ed. by J. Bryant and R.G. Halloway), p. 247, American Association of Stratigraphic Palynologists, Dallas

Gilliam, J.A., Kapp, R.O. & Bogue, R.D. (1967) A post-Wisconsin pollen sequence from Vestaburg Bog, Moncalm County, Michigan. Michigan Academy of Science, Arts and Letters 52, 3–17.

Grimm, E.C. (1983) Chronology and dynamics of vegetation change in the prairie-woodland region of southern Minnesota, U.S.A. New Phytologist 93, 311–350.

Grimm, E.C. (1987) CONISS: a FORTRAN 77 program for stratigraphically constrained cluster analysis by the method of incremental sum of squares. Computers & Geosciences 13, 13–35. https://doi.org/10.1016/0098-3004(87)90022-7

Grubb, P.J. (1977) The Maintenance of Species-Richness in Plant Communities: The Importance of the Regeneration Niche. Biological Reviews 52, 107–145. https://doi.org/10.1111/j.1469-185X.1977.tb01347.x

Haslett, J. & Parnell, A. (2008) A simple monotone process with application to radiocarbon-dated depth chronologies. Journal of the Royal Statistical Society: Series C (Applied Statistics) 57, 399–418. https://doi.org/10.1111/j.1467-9876.2008.00623.x

Ibe, R.A. (1985) Postglacial montane vegetational history around Balsam Lake, Catskill Mountains, New York. Bulletin of the Torrey Botanical Club 112, 176–186.

Jackson, S.T., Betancourt, J.L., Booth, R.K. & Gray, S.T. (2009) Ecology and the ratchet of events: Climate variability, niche dimensions, and species distributions. Proceedings of the National Academy of Sciences of the United States of America 106, 19685–19692. https://doi.org/10.1073/pnas.0901644106

Jackson, S.T. & Blois, J.L. (2015) Community ecology in a changing environment: Perspectives from the Quaternary. Proceedings of the National Academy of Sciences 112, 4915–4921. https://doi.org/10.1073/pnas.1403664111

Juggins, S. (2022) rioja: Analysis of Quaternary Science Data.

839 Maenza-Gmelch, T.E. (1997) Holocene vegetation, climate, and fire history of the Hudson
840 Highlands, southeastern New York, USA. The Holocene 7, 25–37.

841 Marsicek, J.P., Shuman, B., Brewer, S., Foster, D.R. & Oswald, W.W. (2013) Moisture and
842 temperature changes associated with the mid-Holocene Tsuga decline in the northeastern
843 United States. Quaternary Science Reviews 80, 333–342.
844 https://doi.org/10.1016/j.quascirev.2013.09.001

845 Mayle, F.E., Levesque, AndréJ. & Cwynar, L.C. (1993) Alnus as an indicator taxon of the
846 Younger Dryas cooling in eastern North America. Quaternary Science Reviews 12, 295–
847 305. https://doi.org/10.1016/0277-3791(93)90038-N

848 Menking, K.M., Peteet, D.M. & Anderson, R.Y. (2012) Late-glacial and Holocene vegetation
849 and climate variability, including major droughts, in the Sky Lakes region of southeastern
850 New York State. Palaeogeography, Palaeoclimatology, Palaeoecology 353–355, 45–59.
851 https://doi.org/10.1016/j.palaeo.2012.06.033

852 Middleton, A.D. (1973) Johannes Walther's Law of the Correlation of Facies. GSA Bulletin 84,
853 979–988. https://doi.org/10.1130/0016-7606(1973)84<979:JWLOTC>2.0.CO;2

854 Mott, R.J. & Farley-Gill, L.D. (1978) A late-Quaternary pollen profile from Woodstock, Ontario.
855 Canadian Journal of Earth Sciences 15, 1101–1111.

856 Myers, R.E. (1954) The Geology of Bradford County, Pennsylvania. Rocks & Minerals 29, 144–
857 178. https://doi.org/10.1080/00357529.1954.11767008

858 Newby, P., Shuman, B., Donnelly, J.P., Karnauskas, K.B. & Marsicek, J.P. (2014) Centennial-to-
859 Millennial Hydrologic Trends and Variability along the North Atlantic Coast, U.S.A.,
860 during the Holocene. Geophys. Res. Lett. 41. https://doi.org/10.1002/2014GL060183

861 Nowacki, G.J. & Abrams, M.D. (2015) Is climate an important driver of post-European
862 vegetation change in the Eastern United States? Global Change Biology 21, 314–334.
863 https://doi.org/10.1111/gcb.12663

864 Nowacki, G.J. & Abrams, M.D. (2008) The Demise of Fire and "Mesophication" of Forests in
865 the Eastern United States. BioScience 58, 123–138. https://doi.org/10.1641/B580207

866 Oswald, W.W., Doughty, E.D., Foster, D.R., Shuman, B.N. & Wagner, D.L. (2016) Evaluating
867 the role of insects in the middle-Holocene Tsuga decline. The Journal of the Torrey
868 Botanical Society 144, 35–39. https://doi.org/10.3159/TORREY-D-15-00074.1

869 Oswald, W.W., Faison, E.K., Foster, D.R., Doughty, E.D., Hall, B.R. & Hansen, B.C.S. (2007)
870 Post-glacial changes in spatial patterns of vegetation across southern New England.
871 Journal of Biogeography 34, 900–913.

872 Oswald, W.W., Foster, D.R., Shuman, B.N., Chilton, E.S., Doucette, D.L. & Duranleau, D.L.
873 (2020) Conservation implications of limited Native American impacts in pre-contact New
874 England. Nature Sustainability 3, 241–246. https://doi.org/10.1038/s41893-019-0466-0

875 Oswald, W.W., Foster, D.R., Shuman, B.N., Doughty, E.D., Faison, E.K., Hall, B.R., Hansen,
876 B.C.S., Lindbladh, M., Marroquin, A. & Truebe, S.A. (2018) Subregional variability in
877 the response of New England vegetation to postglacial climate change. Journal of
878 Biogeography 45, 2375–2388. https://doi.org/10.1111/jbi.13407

879 Paciorek, C.J., Goring, S.J., Thurman, A.L., Cogbill, C.V., Williams, J.W., Mladenoff, D.J.,
880 Peters, J.A., Zhu, J. & McLachlan, J.S. (2016) Statistically-estimated tree composition for
881 the northeastern United States at Euro-American settlement. PloS one 11, e0150087.

882 Paine, R.T., Tegner, M.J. & Johnson, E.A. (1998) Compounded Perturbations Yield Ecological
883 Surprises. Ecosystems 1, 535–545.

884 Parnell, A.C., Haslett, J., Allen, J.R.M., Buck, C.E. & Huntley, B. (2008) A flexible approach to
885 assessing synchroneity of past events using Bayesian reconstructions of sedimentation
886 history. Quaternary Science Reviews 27, 1872–1885.
887 https://doi.org/10.1016/j.quascirev.2008.07.009

888 Pederson, N., Dyer, J.M., McEwan, R.W., Hessl, A.E., Mock, C.J., Orwig, D.A., Rieder, H.E. &
889 Cook, B.I. (2014) The legacy of episodic climatic events in shaping temperate, broadleaf
890 forests. Ecological Monographs 84, 599–620. https://doi.org/10.1890/13-1025.1

891 Peteet, D.M., Vogel, J.S., Nelson, D.E., Southron, J.R., Nickmann, R.J. & Heusser, L.E. (1990)
892 Younger Dryas climatic reversal in northeastern USA? AMS ages for an older problem.
893 Quaternary Research 33, 219.

894 Peterson, A.T., Soberon, J., Pearson, R.G., Anderson, R.P., Martinez-Meyer, E., Nakamura, M.
895 & Araújo, M.B. (2011) Ecological Niches and Geographic Distributions. Princeton
896 University Press, Princeton, N.J.

897 Poage, N.J. & Peart, D.R. (1993) The Radial Growth Response of American Beech (Fagus
898 grandifolia) to Small Canopy Gaps in a Northern Hardwood Forest. Bulletin of the
899 Torrey Botanical Club 120, 45–48. https://doi.org/10.2307/2996662

900 Prentice, I.C., Bartlein, P.J. & Webb III, T. (1991) Vegetation and climate changes in eastern
901 North America since the last glacial maximum: A response to continuous climatic
902 forcing. Ecology 72, 2038–2056.

903 PRISM Climate Group (2022) http://prism.oregonstate.edu, created December 2022.

904 R Core Development Team (2022) R: A language and environment for statistical computing. R
905 Foundation for Statistical Computing, Vienna, Austria.

906 Ramiadantsoa, T., Stegner, M.A., Williams, J.W. & Ives, A.R. (2019) The potential role of
907 intrinsic processes in generating abrupt and quasi-synchronous tree declines during the
908 Holocene. Ecology 100, e02579. https://doi.org/10.1002/ecy.2579

909 Reber, E.J. (1973) Soil Survey: Susquehanna County, Pennsylvania.

910 Reimer, P.J., Austin, W.E.N., Bard, E., et al. (2020) The IntCal20 Northern Hemisphere
911 Radiocarbon Age Calibration Curve (0–55 cal kBP). Radiocarbon 62, 725–757.
912 https://doi.org/10.1017/RDC.2020.41

913 Sachs, J.P. (2007) Cooling of Northwest Atlantic slope waters during the Holocene. Geophys.
914 Res. Lett. 34, L03609. https://doi.org/10.1029/2006gl028495

915 Schlenker, N., Johnson, J., Ray-Cozzens, T., Nelson, D.M., Shuman, B.N., Stefanova, I. &
916 Williams, J.W. (2024) Interacting effects of fire and hydroclimate on oak and beech
917 community prevalence in the southern Great Lakes region. Journal of Ecology 112,
918 1101–1122. https://doi.org/10.1111/1365-2745.14289

919 Seddon, A.W., Macias-Fauria, M. & Willis, K.J. (2015) Climate and abrupt vegetation change in
920 Northern Europe since the last deglaciation. The Holocene 25, 25–36.
921 https://doi.org/10.1177/0959683614556383

922 Sevon, W.D. (2000) Physiographic Provinces of Pennsylvania, DCNR Map 13.

923 Sevon, W.D. & Braun, D.D. (1997) Glacial Deposits of Pennsylvania, DCNR Map 59.
924 Commonwealth of Pennsylvania, Department of Conservation and Natural Resources,
925 Bureau of Topographic and Geologic Survey.

926 Shuman, B. (2003) Controls on loss-on-ignition variation in cores from two shallow lakes in the
927 northeastern United States. Journal of Paleolimnology 30, 371–385.

928 Shuman, B.N. & Burrell, S.A. (2017) Centennial to millennial hydroclimatic fluctuations in the
929 humid northeast United States during the Holocene. Quaternary Research, 1–11.
930 https://doi.org/10.1017/qua.2017.62

931 Shuman, B.N., Marsicek, J., Oswald, W.W. & Foster, D.R. (2019) Predictable hydrological and
932 ecological responses to Holocene North Atlantic variability. Proceedings of the National
933 Academy of Sciences 116, 5985–5990. https://doi.org/10.1073/pnas.1814307116

934 Shuman, B.N., Newby, P. & Donnelly, J.P. (2009) Abrupt climate change as an important agent
935 of ecological change in the Northeast U.S. throughout the past 15,000 years. Quaternary
936 Science Reviews 28, 1693–1709.

937 Shuman, B.N., Newby, P., Huang, Y. & Webb, T. (2004) Evidence for the close climatic control
938 of New England vegetation history. Ecology 85, 1297–1310.

939 Shuman, B.N., Stefanescu, I.C., Grigg, L., Foster, D.R. & Oswald, W.W. (2023) A Millennial-
940 Scale Oscillation in Latitudinal Temperature Gradients along the Western North Atlantic
941 during the Mid-Holocene. Geophysical Research Letters 50, e2022GL102556.
942 https://doi.org/10.1029/2022GL102556

943 Stefanescu, I.C., Shuman, B.N., Grigg, L.D., Bailey, A., Stefanova, V. & Oswald, W.W. (2023)
944 Weak precipitation δ2H response to large Holocene hydroclimate changes in eastern

North America. Quaternary Science Reviews 304, 107990. https://doi.org/10.1016/j.quascirev.2023.107990

Thompson, J.R., Carpenter, D.N., Cogbill, C.V. & Foster, D.R. (2013) Four Centuries of Change in Northeastern United States Forests. PLOS ONE 8, e72540. https://doi.org/10.1371/journal.pone.0072540

Thompson, R.S., Anderson, K.H. & Bartlein, P.J. (1999) Atlas of Relations Between Climatic Parameters and Distributions of Important Trees and Shrubs in North America. U.S. Geological Survey Professional Paper 1650-B, Denver.

Toney, J.L., Rodbell, D.T. & Miller, N.G. (2003) Sedimentologic and palynologic records of the last deglaciation and Holocene from Ballston Lake, New York. Quaternary Research 60, 189–199. https://doi.org/10.1016/S0033-5894(03)00093-0

Turner, M.G., Baker, W.L., Peterson, C.J. & Peet, R.K. (1998) Factors influencing succession: Lessons from large, infrequent natural disturbances. Ecosystems 1, 511–523.

Turner, M.G., Braziunas, K.H., Hansen, W.D. & Harvey, B.J. (2019) Short-interval severe fire erodes the resilience of subalpine lodgepole pine forests. Proceedings of the National Academy of Sciences 116, 11319–11328.

Turner, M.G., Romme, W.H., Gardner, R.H., O'Neill, R.V. & Kratz, T.K. (1993) A revised concept of landscape equilibruim: Disturbance and stability on scaled landscapes. Landscape Ecology 8, 213.

Tzedakis, P.C. (1992) Effects of Soils on the Holocene History of Forest Communities, Cape Cod, Massachusetts, U.S.A. Géographie physique et Quaternaire 46, 113–124.

USDA Natural Resources Conservation Service (2016) USDA-NRCS Official Soil Series Description.

Watts, W.A. (1979) Late Quaternary vegetation of central Appalachia and the New Jersey coastal plain. Ecological Monographs 49, 427–469.

Webb, T., III (1986) Is vegetation in equilibrium with climate? How to interpret late-Quaternary pollen data. Vegetatio 67, 75–91.

Willard, D.A., Bernhardt, C.E., Korejwo, D.A. & Meyers, S.R. (2005) Impact of millennial-scale Holocene climate variability on eastern North American terrestrial ecosystems: pollen-based climatic reconstruction. Global and Planetary Change 47, 17–35. https://doi.org/10.1016/j.gloplacha.2004.11.017

Williams, J.W., Blois, J.L. & Shuman, B.N. (2011) Extrinsic and intrinsic forcing of abrupt ecological change: case studies from the late Quaternary. Journal of Ecology 99, 664–677. https://doi.org/10.1111/j.1365-2745.2011.01810.x

Williams, J.W., Post, D.M., Cwynar, L.C., Lotter, A.F. & Levesque, A.J. (2002) Rapid and widespread vegetation responses to past climate change in the North Atlantic region. Geology 30, 971.

Williams, J.W., Shuman, B., Bartlein, P.J., et al. (2006) An Atlas of Pollen-Vegetation-Climate Relationships for the United States and Canada. American Association of Stratigraphic Palynologists Foundation, Dallas, TX.

Wood, P.O. (1911) Soil Survey of Bradford County, Pennsylvania.

Yu, Z., Andrews, J.H. & Eicher, U. (1997) Middle Holocene dry climate caused by change in atmospheric circulation patterns: Evidence from lake levels and stable isotopes. Geology 25, 251–254.

990 Table 1. Radiocarbon ages from the Blanding Lake and Sunfish Pond cores

		Depth	Thickness			^{14}C age	Uncertainty		Calibrated age range		
Lake	Core	(top cm)	(cm)	Material	Lab number	(YBP)	(yr)	Accepted	5%	Median	95%
Blanding Lake	555	546	1		Core top	-65	1				
	555	619	2	charcoal	UCI-190318	625	45		550	601	658
	555	679	2	charcoal	UCI-190319	2225	35		2159	2228	2320
	555	796	2	charcoal	UCI-190320	3450	70		3578	3716	3858
	555	873	1	charcoal	UCI-190321	4280	20		4837	4847	4858
	555	913	1	charcoal	UCI-190322	4410	20		4891	4986	5036
	555	1025	2	charcoal	UCI-190323	16300	80	No	19534	19670	19852
	555	1086	1	charcoal	UCI-190324	7230	130		7842	8059	8292
	555	1122	1	charcoal	UCI-190325	7925	50		8631	8765	8963
	555	1198	2	charcoal	UCI-190326	8950	60		9913	10057	10206
	555	1283	1	charcoal	UCI-190327	12080	45		13809	13930	14038
Sunfish Pond	585B	585	1		Core top	-65	1		-67	-65	-64
	585B	671	1	charcoal	OS-127540	650	20		563	588	657
	585B	766	1	bulk sediment	OS-161249	2940	20		3011	3102	3159
	585B	796	1	bulk sediment	OS-161250	3870	25		4187	4304	4397
	585B	812	1	bulk sediment	OS-161251	4650	30	No	5320	5404	5456
	585B	838	1	charcoal	OS-127541	6520	65	No	7317	7427	7549
	585B	915	2	bulk sediment	OS-161275	5710	25		6419	6488	6585
	585B	962	1	bulk sediment	OS-127542	6840	70		7587	7676	7814
	585B	1060	1	bulk sediment	OS-127543	9190	110		10208	10377	10602
	585B	1060	1	bulk sediment	OS-127544	9330	110		10290	10533	10941
	585B	1108	1	bulk sediment	OS-161276	1130	15	No	976	1014	1060
	585B	1215	1	bulk sediment	OS-127545	15650	280	No	18387	18962	19478
	585B	1360	1	bulk sediment	OS-127546	38600	5500	No	34290	42452	52388

991